

# Construction of MBD Models from xEV Vehicle Disassembly Benchmark Data and their Engineering Utilization

Hiroshi SHIMIZU\*<sup>1</sup> · Dr. Kenichi ISHIHARA\*<sup>1</sup> · Motohiro ITADANI · Akira NAKAYAMA\*<sup>1</sup>

\*<sup>1</sup>Computational Science Center, Technology Unit, KOBELCO RESEARCH INSTITUTE, INC.

## Abstract

Many automakers are focusing on developing electric vehicles (EVs). In this effort, benchmarking research, which focuses on the automobiles of competitors and leading companies, is an important process for understanding the latest technology and market trends. Utilizing computer-aided engineering (CAE) in benchmark research allows for various investigations without compromising the research subject. An exemplary CAE model has been created from 3D-shape measurement data of an EV battery pack to perform several evaluations (e.g., impact crushing, thermal runaway, and durability.) The durability issue, herein identified, has been addressed by improving the cross-sectional shape of the components on the basis of the results of topology optimization. As a result, both durability and impact safety have been enhanced.

## Introduction

With automakers' focus on developing electric vehicles (EVs), benchmarking research centering around the automobiles of competitors and leading companies reveals our own products' advantages and opportunities for improvement in comparison with others on the market. Ultimately, this information helps us improve our competitiveness. This research is key to understanding other companies' latest technologies and products and to developing products that are in line with market trends and customer requirements.

One challenge, though, is that destructive testing processes (e.g., durability and crush testing) limit the number of devices under test because of high procurement costs. However, by using computer aided engineering (CAE) for reverse engineering, it is possible to run multiple tests without causing wear to parts.

In 2021, Kobelco Research Institute, Inc. began conducting disassembly benchmarking research into the latest EV vehicles made outside Japan. Data on performance, structural, and physical properties for each of the vehicles' components are compiled into reports available for commercial purchase. As part of the process, we create model-based development (MBD) models, CAD models, and finite element

analysis (FEA) data based on the research data. This paper describes how 3D models based on disassembly benchmarking data for battery packs can be used in engineering design. Use cases covered include the durability evaluation of battery packs, collision safety, and thermal runaway evaluation, and topology optimization of the internal structure of battery cases.

## 1. Battery pack modeling

3D data of component geometry (CAD data) is needed to create the numerical analysis model of a battery pack for collision safety evaluation. We used a handheld non-contact scanner (accuracy up to 0.050 mm) to measure geometry while disassembling the battery pack of an EV produced by a non-Japanese manufacturer. We used these data to model the surface for the CAD model. Fig. 1 shows the actual battery packs, their scanned shapes, and the surfaced CAD data. The scope of the CAD data was limited to structural components that contribute to collision safety performance. We used the CAD

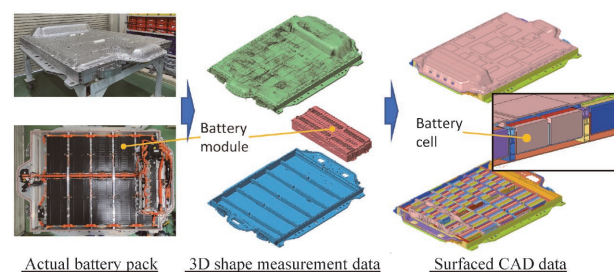


Fig. 1 Creating CAD data for the actual battery pack

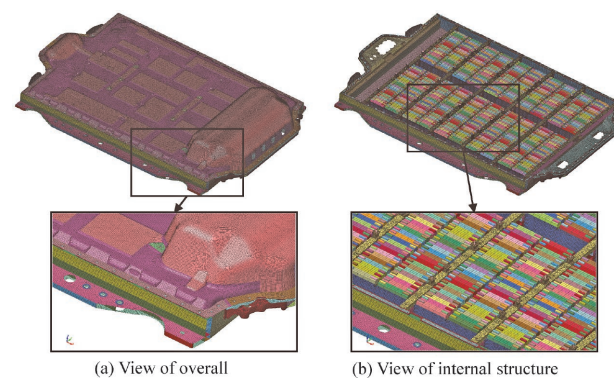


Fig. 2 Mesh model for the numerical simulation

data to create a mesh model for CAE, as shown in Fig. 2, and performed numerical analysis to evaluate safety and durability. The model comprised about 1.3 million nodes and 1.5 million elements.

## 2. Durability evaluation via CAE

ISO 12405 specifies standard tests for the durability evaluation of battery packs.<sup>1), 2)</sup> One of the reliability tests in this standard is a vibration test, which determines whether battery damage or faulty electrical contact could result from random oscillations caused by vehicle travel or drivetrain vibration. Fig. 3 shows a power spectral density (PSD) chart per ISO 12405. Although the ISO 12405 vibration test method is based on vibration data from driving in Germany, it has been validated as applicable to road conditions in Japan.<sup>3)</sup> Alternatively, random response analysis is an efficient and relatively quick method for running simulated testing for vibration caused by random waves.<sup>4)</sup> We used this method for the durability evaluation of battery packs because of its reasonable computational cost and applicability to design. MSC Nastran, a multidisciplinary vibration and structural analysis program, was used as the analysis solver. Fig. 4 shows the analysis conditions for random response analysis. Since the battery pack is bolted to the side sill and floor, this is the transmission path for vibration. Therefore, the bolted joints were rigidly coupled with rigid 1D elements, and all bolted joints were vibrated simultaneously. Fig. 3 shows the PSD results upon simultaneous excitation in the three axes of front-back, side-to-side, and up-down. Fig. 5 shows the stress RMS (root mean square) contour plot from the random response analysis. Stress RMS indicates the average variation in stress in terms of a random response and is an index for statistically evaluating a structure's response to random load.<sup>5)</sup>

Results show that the stress is at its maximum at the bolted joint, with a stress RMS of 133 MPa. This exceeds the fatigue strength  $\sigma_w$  ( $10^7$  cycles) of extruded 6N01-T5, which is 108 MPa<sup>6)</sup>. There is a distinct peak in stress PSD at 43 Hz. Stress PSD is an index for the power distribution of random stress acting on a structure for a given frequency.<sup>7)</sup> Specifically, it represents the spectral density obtained by Fourier transformation of the time-history data of stress. Fig. 6 shows the results of natural vibration analysis performed to determine the vibration mode of 43 Hz. The first-order vibration mode of the battery pack occurs at 43 Hz, coinciding with the frequency of the peak stress PSD.

Although this vibration mode causes bending

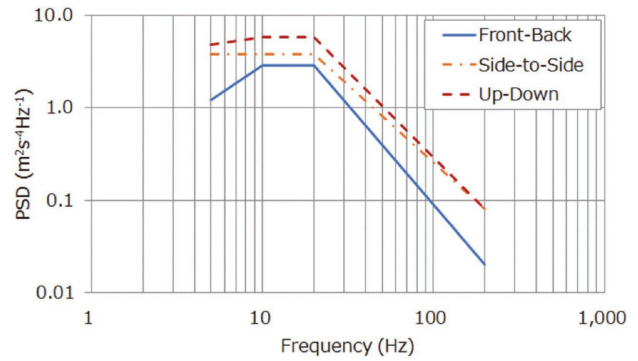


Fig. 3 PSD on 3 axes with ISO 12405

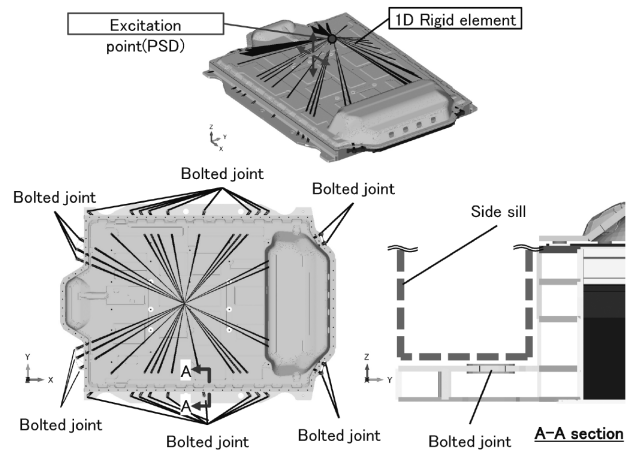


Fig. 4 Analysis conditions for random response analysis

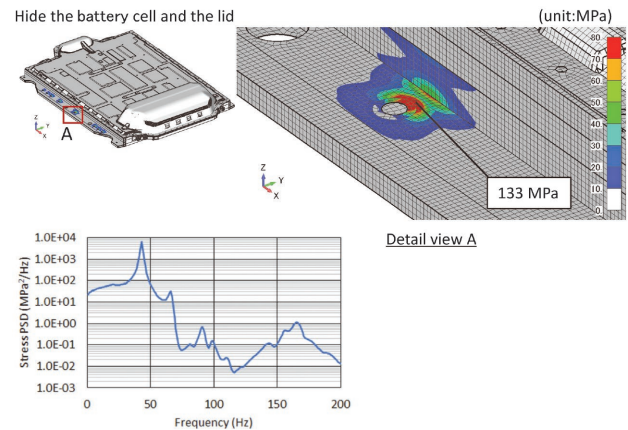


Fig. 5 Stress RMS value contour for random response analysis

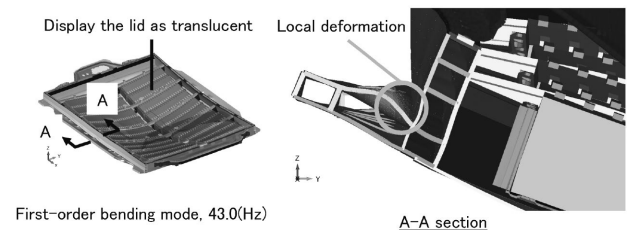


Fig. 6 Natural vibration modes of first-order bending

deformation throughout the entire battery pack, the degree of local deformation is particularly high near the bolted joints. As such, increasing surface rigidity at the bolted joints should be an efficient way to reduce stress.

### 3. Using CAE for collision safety evaluation

Standards for vehicle collision safety evaluation vary by country and region. Collision safety minimizes harm to pedestrians and vehicle occupants in the event of an automobile accident. Impact tests are typically performed for three main directions: front, side, and rear. However, with EVs, there is a risk of fire due to thermal runaway of the lithium-ion battery, meaning it is vital to account for the collision safety of the battery pack itself. This led us to use numerical analysis to validate the collision deformation performance, specifically of the battery pack. We used the side impact test to validate performance, as this is the direction in which collision deformation is most likely to be transmitted to the battery pack. **Fig. 7** shows the impact conditions simulating the impact of a pole on the side of the battery pack.

Although the original intention behind collision safety applies to the frame, we analyzed the collision phenomena of the battery pack in isolation to understand this component's design in terms of collision resistance. In this study, we evaluated whether safety is maintained upon absorbing the kinetic energy generated by the mass of the battery pack.

Impact speeds were 32 km/h as referred to in UN Regulation (UN-R135), "pole side-impact protection," and approximately twice this value as an excessive condition, at 60 km/h. We used the multidisciplinary program Ansys LS-DYNA (hereafter, LS-DYNA) as the analysis solver.

**Fig. 8** shows the deformation condition of the battery pack at an impact speed of 32 km/h. The side frame of the battery pack curves toward the interior at the pole's area of impact. Deformation is confined to the area between the side frame and the battery module and does not affect the battery module. This result indicates that this location was intended as a crumple zone to ensure safety by preventing frame deformation from reaching the battery cells upon side impact.

Next, we tested the impact conditions beyond those stipulated by UN-R135. **Fig. 9** shows the deformation condition of the battery pack at an impact speed of 60 km/h. In a 60-km/h impact, deformation of the side frame reaches the battery module, compressing cells at the edge. Therefore, the

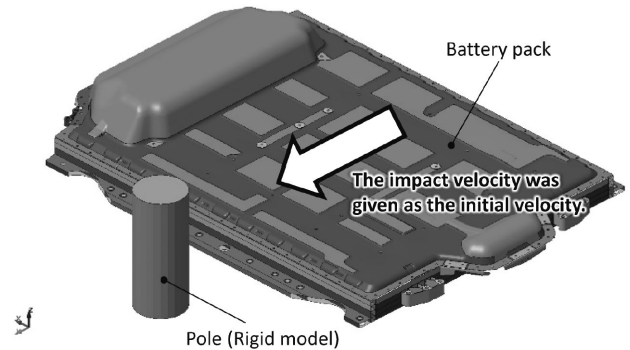


Fig. 7 Battery pack side impact conditions

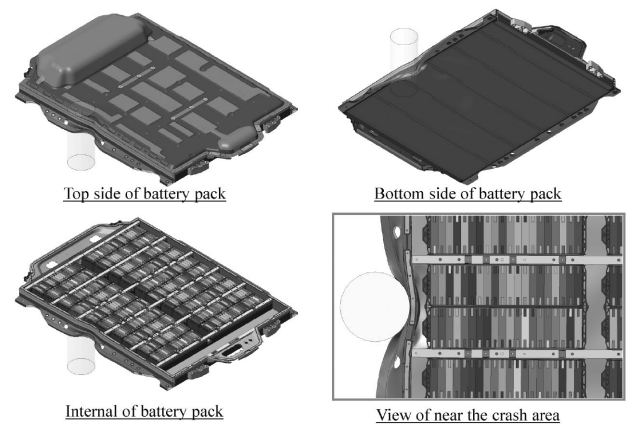


Fig. 8 The deformation condition at an impact speed of 32 km/h

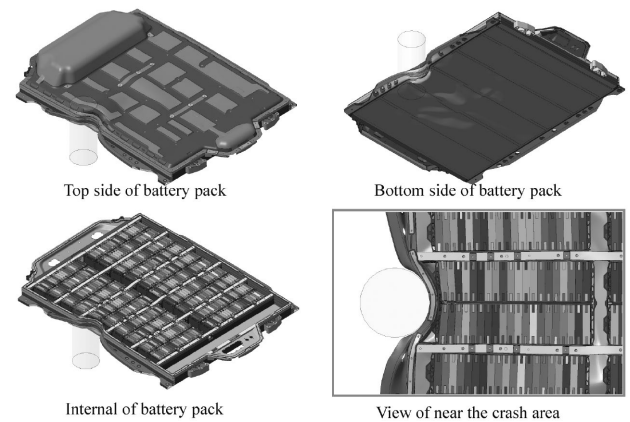


Fig. 9 The deformation condition at an impact speed of 60 km/h

crumple zone does not fully absorb the deformation.

The kinetic energy of a 60 km/h impact is approximately four times that of a 32 km/h impact. The resulting compression could cause a short circuit in the battery cells, resulting in thermal runaway. This battery pack has spaces between each module in the center of the pack, similar to the spaces on the sides, distributed in the side-to-side direction of the frame. Therefore, the design appears to be such that deformation that reaches a module from

the side is absorbed by the rigid body movement of the module itself (sliding movement - Fig. 9, lower right), reducing load on the cells.

#### 4. Evaluating thermal runaway due to short circuiting via CAE

We used LS-DYNA's coupled solver for structure, heat transfer, and electromagnetic (EM) analysis to simulate thermal runaway caused by a short circuit. A short circuit occurs in the battery when the cathode and anode come in direct contact with each other following impact or insulation damage. This causes a sharp rise in current flow inside the battery and therefore an increase in temperature. Thermal runaway is a phenomenon in which the temperature inside the battery rises rapidly and uncontrollably. It can be caused by overcharging, an internal short circuit, or excessive external heat. As thermal runaway progresses, the stored energy is released all at once, causing the battery to overheat, which can lead to a fire or explosion.

Conventional simulations for evaluating battery performance and safety require detailed modeling of each layer of the cell; analyzing such large models is costly. However, there is a method that uses what is called the Battery Macro model (BatMac model<sup>8</sup>). This model represents battery cells with very few meshes, which is beneficial when analyzing many cells or the entire battery. In the BatMac model, a Randles-type equivalent circuit<sup>9</sup> (Fig.10) is accounted for at each node. We used the BatMac model because it can efficiently represent phenomena such as internal short circuits and thermal runaway.

As explained, short circuits and thermal runaway are complex phenomena caused by reactions in a cell. Because heat transfer/EM analysis takes longer than a general quick impact analysis, running a series of coupled analyses is costly. Therefore, for this simulation, we set the deformation and strain conditions from the impact analysis as the initial conditions for the heat transfer/EM analysis. Further, we modeled the short circuit based on the initial strain distribution, and the thermal runaway based on the temperature change after the short circuit. In

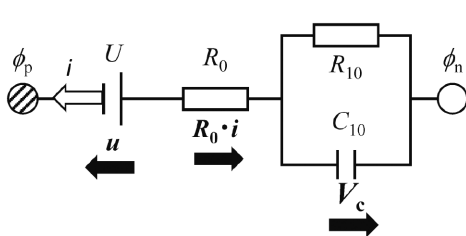


Fig.10 Randles-type equivalent circuit

this way, we were able to run the simulation in a practical time frame.

#### 4.1 Analyzing individual cells

We simulated thermal runaway due to short circuiting in an individual cell using the BatMac model. We applied the same mechanical properties as in the impact analysis and used typical physical property values for each component for the heat transfer and electrical properties. Measured values were used for the cell capacity (57 Ah) and the relationship between voltage and State of charge (hereafter, SOC) (Fig.11). The parameters of the Randles-type equivalent circuit were established as  $R_0 = R_{10} = 0.001$  and  $C_{10} = 1000$  based on charge/discharge curves. As it is not possible to confirm the exact short circuit threshold via testing or other methods, this was assumed to be 10% of the strain of the cell, based on the strain distribution from the impact analysis. We assumed a threshold value of 200°C for thermal runaway based on the temperature at which a typical lithium-ion battery experiences thermal runaway<sup>10</sup>.

Fig.12 shows the initial strain distribution and Joule heat distribution. The figures show that in the region where strain exceeds 10%, short circuiting occurs, causing high current to flow throughout the cell. This leads to high Joule heating throughout the entire cell, including in the non-short-circuited region.

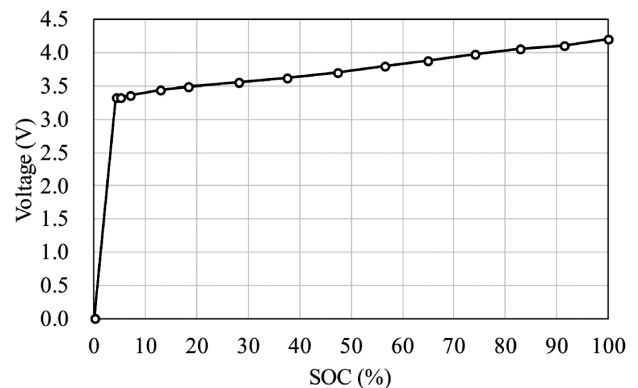


Fig.11 Relationship between voltage and SOC

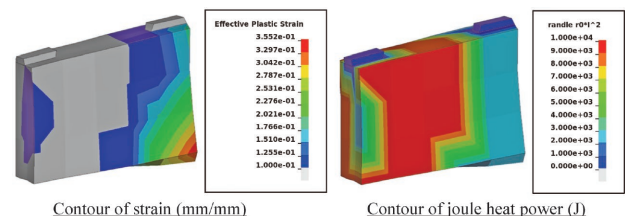


Fig.12 Initial strain distribution and joule heat power distribution of cell

Fig.13 shows the temperature history between the tabs on top of the cell. Deformation causes a short circuit, causing the temperature to rise suddenly, surpassing 200°C just under 40 seconds later due to thermal runaway. The temperature increase stops after a certain amount of heating, ending the thermal runaway. In this way, it is possible to use the BatMac model to simulate the phenomenon of thermal runaway due to short circuiting.

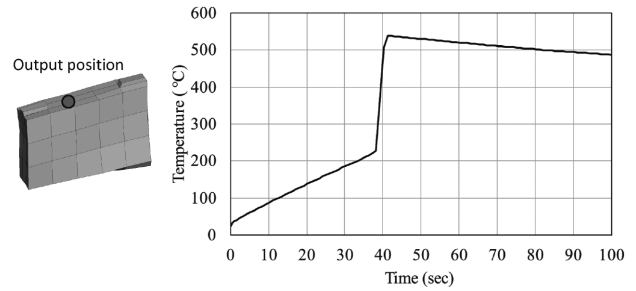


Fig.13 Temperature history between cell top tabs

## 4.2 Analyzing battery packs

We simulated thermal runaway due to short circuiting based on the analysis results for an impact speed of 60 km/h in Section 3, using the parameters set in Section 4.1 for the battery pack. We considered heat transfer by conduction within the cells and between each component as well as heat transfer by convection with the air around the battery pack.

The initial strain and current distributions in Fig.14 show that the strain induced by the impact extends to the second cell from the impact zone (②, left side of the figure). Just like in the analysis of an individual cell, this indicates high current flow in the short-circuited region.

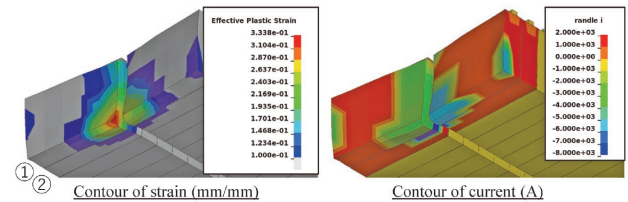


Fig.14 Initial strain distribution and current distribution of module

Fig.15 shows the temperature history between the top tabs of the representative cells (①, ⑤, ⑩, ⑮, ⑳). The temperature of the first cell from the impact zone (①) increased immediately after the start of the short circuit, and thermal runaway occurred when the temperature exceeded 200°C. The temperature of the fifth cell (⑤, dash-dotted line) started to increase about 120 seconds after the impact and rapidly increased about 150 - 160 seconds after the impact. When thermal runaway due to short circuiting occurred in a cell at the impact zone, the phenomenon cascaded to cells far from the impact zone by thermal conduction. 480 seconds later, the thermal runaway was occurring in an entire module.

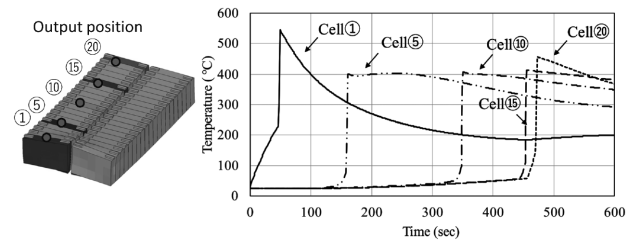


Fig.15 Temperature history between top tabs of representative cells

Fig.16 shows the temperature distribution for specified elapsed times from the start of the short circuit. 50 seconds after the start of the short circuit, the temperature increased in the first and second cells from the impact zone. 473 seconds after the start of the short circuit, the temperature increase affected nearly the entire module. Since the temperature increased only in one module, it is assumed that the structure of the battery pack studied prevents heat transfer between modules.

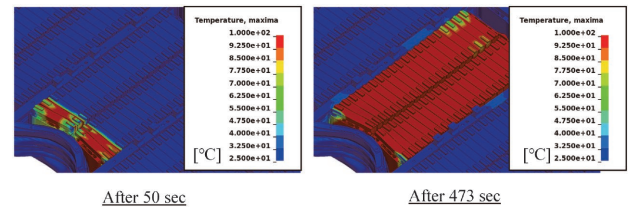


Fig.16 Temperature contour of the module at representative time

As described previously, the BatMac model makes it possible to analyze thermal runaway due to short circuiting for the entire battery pack at a practical cost.

## 5. Optimizing design via CAE

### 5.1 Optimizing extrusion shape

Section 2 covered the occurrence of stresses exceeding the fatigue strength of constituent materials in the durability evaluation. We performed a topology optimization analysis to investigate countermeasures to these stresses. Topology optimization is a structural optimization method that determines the optimal layout while reducing material from the design region given structural constraints, loads, and restraint conditions. To perform this analysis, we used Altair OptiStruct, a general-purpose solver for optimization analysis.

We focused on the side frames and cross members as optimization regions. These are the main structural members with a major influence on the first-order vibration mode of the battery pack. **Fig.17** shows the substructure model for topology optimization. The analysis model was created by partially extracting the side frame and cross member and applying geometric symmetry to create a 1/4 symmetrical model. **Fig.18** shows the design region (pale blue), boundary conditions, and topology optimization results. The design region is the area inside the external surface of the original structure. The original rib arrangement was maintained, and the minimum remaining plate thickness was set to 1 mm, with exceptions where necessary for functionality. As constraint conditions, the areas near bolted joints were fixed, and a load was applied to the top surface of the cross member to express the first-order bending deformation mode. The constraints for the side frame and cross member were that the mass should be the same or lower and that rigidity should be maximized (deflection of the cross member should be minimized).

Topology optimization indicated that a rib should be added to the side frame to connect the

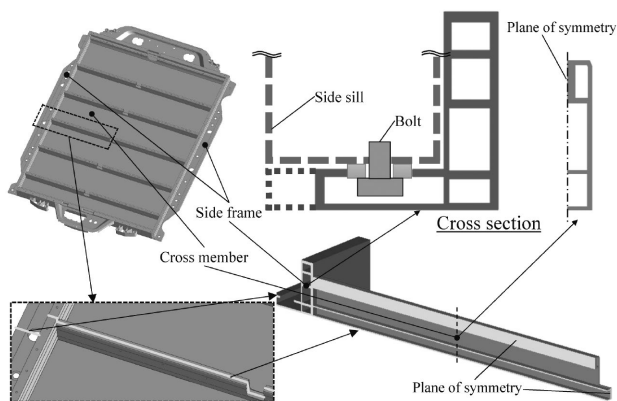


Fig.17 Substructure model for topology optimization

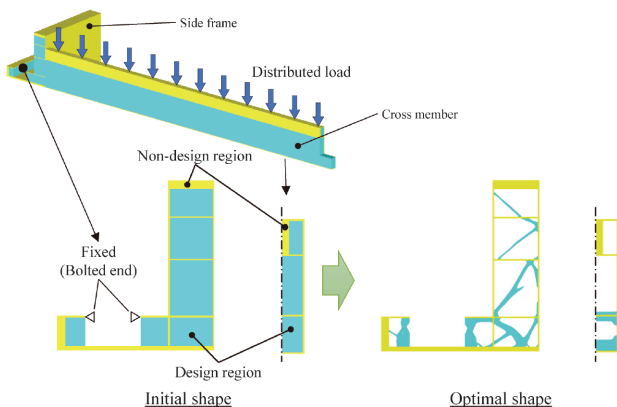


Fig.18 Design region, boundary conditions, and optimization results

upper and lower plates near the bolted joint, that the bolted joint that was previously only on the top surface should also be incorporated on the bottom surface, and that the two lower ribs of the cross member should be thicker. The structural modification shown in **Fig.19** was made based on these results. After the structural modification, the mass of the battery case increased by only 120 g, which is remarkably close to the mass of the original structure.

## 5.2 Durability evaluation

**Fig.20** shows the results of random response analysis applied to the optimized shape from Section 5.1. The maximum stress RMS at the bolted joint was 87 MPa. This constitutes a 35% reduction from the original shape and is below the fatigue strength  $\sigma_w$  ( $10^7$  cycles) of extruded 6N01-T5, which is 108 MPa<sup>5)</sup>. By changing to the optimized shape, the peak stress PSD decreased and shifted to the high-frequency side. **Fig.21** shows the results of natural frequency analysis for the optimized shape. The natural vibration of first-order bending of the battery pack increased by 10%, from 43.0 Hz to 47.3 Hz. The optimized shape suppresses local deformation by the joining of two plates. These results suggest that there are two reasons the optimized shape

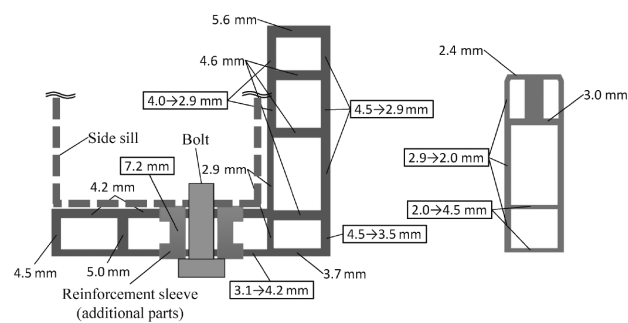


Fig.19 Structural modification proposal based on topology optimization results

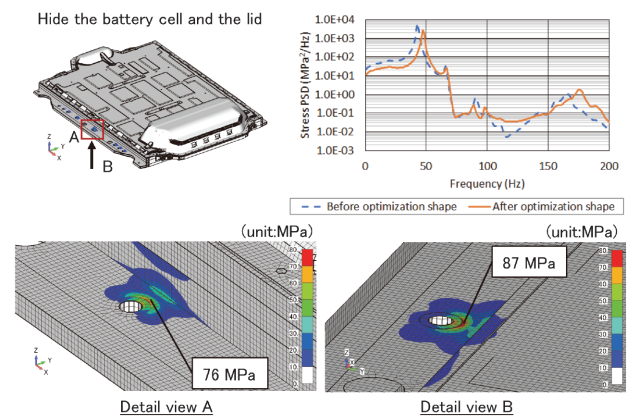


Fig.20 Contour plot of stress RMS values after optimization

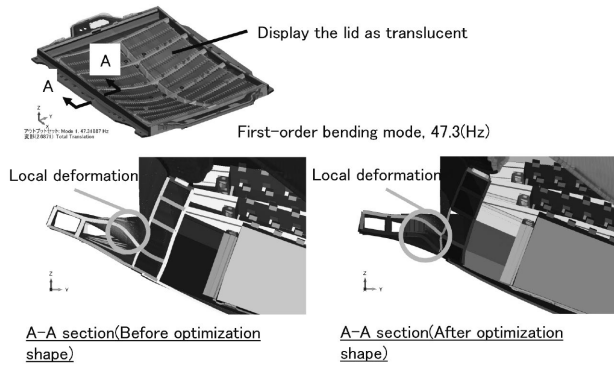


Fig.21 Natural vibration modes of first-order bending after optimization

reduces the stress RMS. The first is the increased rigidity of the bolted surfaces from bolting the two plates together, and the second is the reduced input excitation PSD due to the increase in the natural vibration. Above 20 Hz, PSD decreases as frequency increases (Fig. 3), meaning that as natural frequency increases, input excitation PSD decreases, reducing stress.

This study proves that it is possible to efficiently optimize cross-section geometry in terms of durability without relying on an individual's expertise.

### 5.3 Collision safety evaluation

Fig.22 shows the results of the same impact analysis as in Section 3 (impact speed 32 km/h) applied to the optimized shape from Section 5.1. Increasing the thickness of the plate under the bolted joint from 3.1 mm to 4.2 mm significantly increased impact absorption capacity and decreased side frame deformation. Therefore, this structural modification improved collision safety.

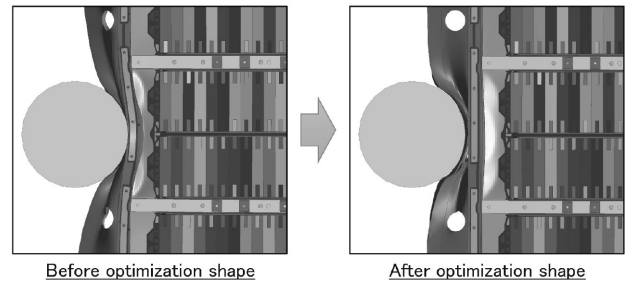


Fig.22 The deformation condition at an impact speed of 32 km/h after optimization

## Conclusions

This paper describes engineering design considerations for battery packs in terms of durability evaluation, collision safety evaluation, evaluation of thermal runaway due to short circuiting, and design optimization using CAE. Using CAE in disassembly benchmarking research is very effective for comparing performance with other companies' products and understanding design trends. It enables quick feedback during the design phase and improves efficiency within the development process.

## References

- 1) ISO 12405-1:2011: Electrically propelled road vehicles - Test specification for lithium-ion traction battery packs and systems. Part 1: High-power applications.
- 2) ISO 12405-2:2012: Electrically propelled road vehicles - Test specification for lithium-ion traction battery packs and systems. Part 2: High-energy applications.
- 3) K. Maeda et al. Proceedings of the Society of Automotive Engineers of Japan, Inc. 2015, Vol.46, No.1, pp.109-114.
- 4) M. Itadani et al. Kobelnics. 2023, Vol.31, No.57, pp.23-29.
- 5) S. Fujita et al. FUJITSU TEN Technical Journal. 2016, Vol.33, No.1, p.45.
- 6) Japan Aluminum Association. Aluminum Handbook. 7th edition. shoehisa Co. Ltd. 2007, p.57.
- 7) N. Takeda et al. Journal of the Society of Materials Science, Japan. 2012, Vol.61, No.10, p.853.
- 8) LST, an Ansys company. LS-DYNA Keyword User's Manual Volume III. Multi-Physics Solvers. LS-DYNA R13.
- 9) P. L'Eplattenier et al. 12th European LS-DYNA Conference. 2019.
- 10) T. Mukai et al. Journal of The Surface Finishing Society of Japan. 2019, Vol.70, No.6, pp.301-307.